UV Solar-Blind-Region Phase-Matchable Optical Nonlinearity and Anisotropy in a π-Conjugated Cation-Containing Phosphate

Chao Wu,[a],† Xingxing Jiang,[b],† Zujian Wang,[c],† Hongyuan Sha,[c] Zheshuai Lin,[b] Zhipeng Huang,[a] Xifa Long,[c] Mark G. Humphrey,[d] and Chi Zhang*[a]

[a] Dr. C. Wu, Prof. Z. P. Huang, Prof. C. Zhang
China-Australia Joint Research Center for Functional Molecular Materials, School of Chemical Science and Engineering, Tongji University, Shanghai 200092, China
E-mail: chizhang@tongji.edu.cn
[b] Dr. X. X. Jiang, Prof. Z. S. Lin
Technical Institute of Physics and Chemistry, Chinese Academy of Sciences, Beijing 100190, China
[c] Dr. Z. J. Wang, H. Y. Sha, Prof. X. F. Long
Key Laboratory of Optoelectronic Materials Chemistry and Physics, State Key Laboratory of Structure Chemistry, Fujian Institute of Research on the Structure of Matter, Chinese Academy of Sciences, Fuzhou, Fujian 350002, China
[d] Prof. M. G. Humphrey
Research School of Chemistry, Australian National University, Canberra, ACT 2601, Australia
[†] These authors contributed equally to this work

Supporting information for this article is given via a link at the end of the document.

Abstract: Wide ultraviolet (UV) transparency, strong second-harmonic generation (SHG) response, and sufficient optical birefringence for phase-matching (PM) at short SHG wavelengths are three vital prerequisites for practical UV nonlinear optical (NLO) materials. However, simultaneously optimizing these properties remains a major challenge, particularly for metal phosphates, due to their competing requirements. Herein, we report a non-traditional π-conjugated cation-based UV NLO phosphate $[C(NH_2)_3]_6(PO_4)_2{\cdot}3H_2O$ (GPO) with a short UV cutoff edge. Remarkably, GPO is not only SHG active at 1064 nm (3.8 × KH_2PO_4 @ 1064 nm) and 532 nm (0.3 × β-BaB_2O_4 @ 532 nm), but it also possesses the largest birefringence (0.078 @ 546 nm) among phosphates with a band gap exceeding 6.0 eV. The PM SHG capability of GPO can extend to 250 nm, indicating GPO is a promising UV solar-blind NLO material. Theoretical calculations and crystal structure analysis demonstrate that the rare coexistence of wide UV transparency, large SHG response and optical anisotropy can be attributed to the introduction of the π-conjugated cations $[C(NH_2)_3]^+$ and their favorable arrangement with $[PO_4]^{3-}$ anions.

Nonlinear optical (NLO) crystals capable of extending the wavelength range of solid-state lasers to the ultraviolet (UV) region are critically important for a variety of significant applications such as laser medical treatment, material micromachining, and photolithography.[1-3] In the past decades, the search for UV NLO materials has mostly focused on π-conjugated anionic systems,[4,5] the resultant materials including commercialized borates β-BaB_2O_4 (β-BBO),[6a] LiB_3O_5 (LBO),[6b] and $KBe_2BO_3F_2$ (KBBF),[6c] as well as the newly developed fluorooxoborates $NH_4B_4O_6F$[7a] and $Ca_2B_{10}O_{14}F_6$.[7b] It has proven to be extremely challenging to create the ideal UV NLO crystal with superior comprehensive optical performance. This is mainly due to the difficulty in optimizing wide UV transparency (also covering the UV solar-blind (200-280 nm) or even deep UV (< 200 nm) regions), a large second-harmonic generation (SHG) coefficient (> d_{36} (KH_2PO_4 (KDP)) = 0.39 pm/V), and sufficient birefringence (Δn > 0.07) for phase-matching (PM) at short SHG wavelengths,[8] attributed to their often-competing structural requirements.

Phosphates have attracted attention as UV NLO material candidates because the $[PO_4]^{3-}$ group does not absorb in the short-wavelength UV region.[9-12] Notable examples include the long-established and commercially available KDP,[10] as well as the recently developed $Ba_3P_3O_{10}X$ (X = Cl, Br),[11a] $Ba_2NaClP_2O_7$,[11b] $K_4Mg_4(P_2O_7)_3$,[11c] and $LiCs_2PO_4$.[11d,e] Unfortunately, owing to the small hyperpolarizability and polarizability anisotropy of the σ bonded $[PO_4]$ tetrahedron,[12] the SHG responses and/or birefringences of most metal phosphates are not demonstrably superior to those of traditional UV π-conjugated anionic systems, such as borates,[13] carbonates,[14] and nitrates[15]. One strategy to enhance SHG response and birefringence is to introduce species exhibiting second-order Jahn−Teller (SOJT) distortion such as d^0 transition metal cations (e.g. Ti^{4+}, W^{6+}, Mo^{6+}),[10,16] stereochemically active lone-pair (SCALP) cations (e.g. Pb^{2+}, Sb^{3+}, Bi^{3+} etc.),[17] and d^{10} configuration cations (e.g. Hg^{2+}, Zn^{2+}, etc.).[18] However, the use of these metal cations usually results in a red shift in the UV cutoff edge, rendering the material unsuitable for UV NLO applications.

Anionic group theory suggests that π-conjugated anionic units are highly desirable structural features for UV NLO materials.[19] In contrast, the potential of π-conjugated cations as UV SHG-active units is thus far essentially unexplored. In the present study, we propose to introduce the π-conjugated cation $[C(NH_2)_3]^+$ into phosphates to improve the linear and nonlinear optical properties. Unlike SOJT cations,[16,17] the strong covalent bonds of the π-conjugated cation $[C(NH_2)_3]^+$ can facilitate a relatively wide UV transparency, with potential applications as UV solar-blind or deep-UV NLO materials. In contrast to common alkali and alkaline-earth metal cations, $[C(NH_2)_3]^+$ possesses a trigonal planar geometry and π-conjugated molecular orbitals,[20] and this may afford a large second-order susceptibility and strong optical anisotropy. The 3D organization of SHG-active tetrahedral anions such as $[PO_4]^{3-}$ can in principle be controlled by π-conjugated cations, potentially leading to optimized polarizability and optical anisotropy when the anions are uniformly aligned, and thereby enhancing SHG response and birefringence simultaneously. We report herein the construction of the UV solar-blind-region NLO phosphate

$[C(NH_2)_3]_6(PO_4)_2{\cdot}3H_2O$ (GPO) containing the π-conjugated cation $[C(NH_2)_3]^+$ and show that it exhibits large ultraviolet linear and nonlinear optical properties – a wide UV transparency (covering the UV solar-blind region), strong SHG responses in both the visible (3.8 × KDP @ 1064 nm) and UV (0.3 × *β*-BBO @ 532 nm) spectral ranges, and a large birefringence (0.078 @ 546 nm) and PM SHG capability extending to 250 nm. First-principles calculations demonstrate the key contribution of the π-conjugated cation $[C(NH_2)_3]^+$ in significantly improving the optical responses of phosphates.

Millimeter-size pure-phased GPO crystals were obtained by a facile aqueous solution-evaporation method in high yield (85%) (Figure S1), the phase purity being confirmed by powder XRD diffraction (Figure S2). GPO shows no decomposition or hygroscopicity upon standing in air at room temperature for three months and is insoluble in several organic solvents, such as ethanol, methanol, acetone, n-hexane. TGA-DSC analysis indicates that GPO is stable at temperatures up to 100 °C, with weight loss occurring in two steps over the range 100−700 °C under a nitrogen atmosphere (Figure S3). In the first step, the weight loss of ca. 8.98% in the range 100−190 °C corresponds to the removal of three molecules of water from the crystal (calculated value 8.93%). The second-step weight loss of about 66.91% (calculated value 67.59%) in the range 190−700 °C can be assigned to the decomposition of the organic cation $[C(NH_2)_3]^+$ and the inorganic anion $[PO_4]^{3-}$. The final weight is 24.11% (calculated value 23.48%), indicating GPO may decompose into P_2O_5 beyond 700 °C.

GPO crystallizes in the noncentrosymmetric polar monoclinic space group *Cc* (No. 9, Tables S1−S4). Its structure features the electroneutral $\{[C(NH_2)_3]_6(PO_4)_2{\cdot}3H_2O\}_\infty$ in a pseudo-three-dimensional framework, comprising $[C(NH_2)_3]$ planar triangles, $[PO_4]$ tetrahedra, and H_2O, interconnected through N−H···O and O−H···O hydrogen bonds (Figure 1). The GPO structure bears a remarkable resemblance to UV NLO metal phosphates except for the three following crucial differences: (1) Metal cations (e.g. Bi^{3+}, Pb^{2+}, Sb^{3+}) are responsible for the UV cutoff edges of the latter (which exhibit cutoff wavelengths generally longer than 280 nm) owing to their lone-pair electrons, whereas in GPO, the UV cutoff edge is significantly blue-shifted due to the strong covalent bonds of $[C(NH_2)_3]^+$. (2) The cationic unit $[C(NH_2)_3]^+$ is isoelectronic with π-conjugated anionic groups and displays a correspondingly large hyperpolarizability and optical anisotropy; this is in stark contrast to NLO-inactive alkali/alkaline-earth metal cations. Two orientations of $[C(NH_2)_3]^+$ are observed in the GPO structure: the $[C(1)(NH_2)_3]$ and $[C(2)(NH_2)_3]$ planar triangles are canted from the (010) crystal plane (dihedral angles 36.2° and 31.5°, respectively). The alignment of the other four $[C(NH_2)_3]$ planar triangles is almost ideal, with the (100) projection of the C−N bond essentially collinear with the *c* axis (angles of deviation 0−7°: Figure 1). Because the SHG response and birefringence are closely related to the arrangement of the polar and anisotropic units, the favorable orientations of the $[C(NH_2)_3]^+$ groups makes a crucial contribution to the enhancement of linear and nonlinear optical responses. (3) The 3D organization of $[PO_4]^{3-}$ anions is usually controlled by metal cations by means of M−O bonds in typical UV NLO metal phosphates, but in GPO, the π-conjugated cation $[C(NH_2)_3]^+$ plays a key role in aligning the $[PO_4]^{3-}$ groups uniformly along the *c* axis via hydrogen bonds,

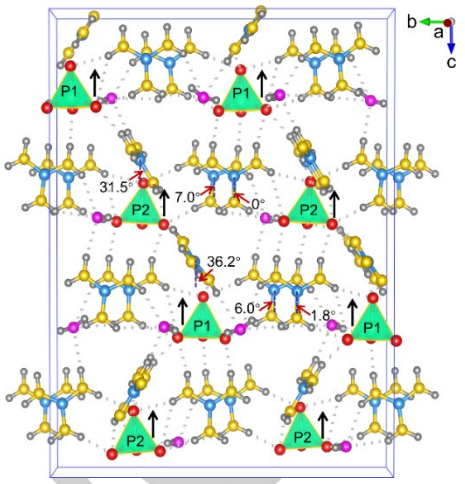

Figure 1. Arrangement of $[C(NH_2)_3]^+$ units and $[PO_4]^{3-}$ groups within one unit cell in GPO. The black arrows represent the orientation of the $[PO_4]^{3-}$ groups.

an ordered arrangement that is very beneficial for the large birefringence and SHG response.

The UV transmittance spectrum of an unpolished GPO crystal (4.8 mm × 0.9 mm × 0.6 mm) afforded a UV cutoff edge of 205 nm (corresponding to 6.05 eV: Figure 2a). The wide band gap indicates that GPO may exhibit a high laser damage threshold. The electronic band structure of a GPO crystal is shown in Figure 2b, with a calculated energy band gap of 4.87 eV. As anticipated, the indirect band gap is underestimated compared to the experimental value, due to the discontinuity of the exchange-correlation function.[21] The calculated partial densities of states reveal that the N-2p, C-2p, and H-1s orbitals make the main contributions to the bottom of the conduction band (CB), while the top of the valence band (VB) primarily originates from N-2p and O-2p orbitals, indicating that the optical band gap of GPO is mainly due to the π-conjugated $[C(NH_2)_3]^+$ cations (Figure 2c).

The SHG efficiency of GPO was measured towards both 1064 and 532 nm laser irradiation using the powder SHG technique. GPO is SHG active at both 1064 nm and 532 nm, with efficiencies of 3.8 × KDP and 0.3 × *β*-BBO, respectively, in the 105−150 *μ*m particle size range (Figures 2e and 2g); the SHG response at 1064 nm is the largest to date for PM UV NLO phosphates with a band gap exceeding 6.0 eV (Table S5). GPO can also realize phase-matching in both the visible and UV regions (Figures 2d and 2f). The phase-matching capability of GPO extends into the UV solar-blind region (*e.g.*, SHG @ 532 nm), which is rare for NLO phosphates. To explore this further, SHG coefficients (d_{ij}) of GPO have been calculated from first-principles.[22] Under the restriction of Kleinman symmetry, the six independent nonzero SHG coefficients are d_{11} = 0.119 pm/V, d_{12} = 0.038 pm/V, d_{13} = −0.063 pm/V, d_{15} = −0.085 pm/V, d_{24} = −0.754 pm/V, and d_{33} = 0.827 pm/V (Table S6).[23] The largest SHG coefficient d_{33} (4.5 × KDP (0.39 pm/V)) is consistent with the experimental result. The contributions to the SHG response from the constituent units were calculated based on the real-space atom-cutting technique (Table S6). The largest SHG coefficient for GPO (d_{33}) largely derives from the $[C(NH_2)_3]^+$ units, which is further confirmed by the calculated percentages of SHG contributions from $[C(NH_2)_3]^+$ (60.2%) and $[PO_4]^{3-}$ (33.8%). An SHG-weighted electron density analysis was also performed on GPO, to intuitively depict the electron clouds of the individual groups dominating the SHG responses (Figures 2h and 2i). The

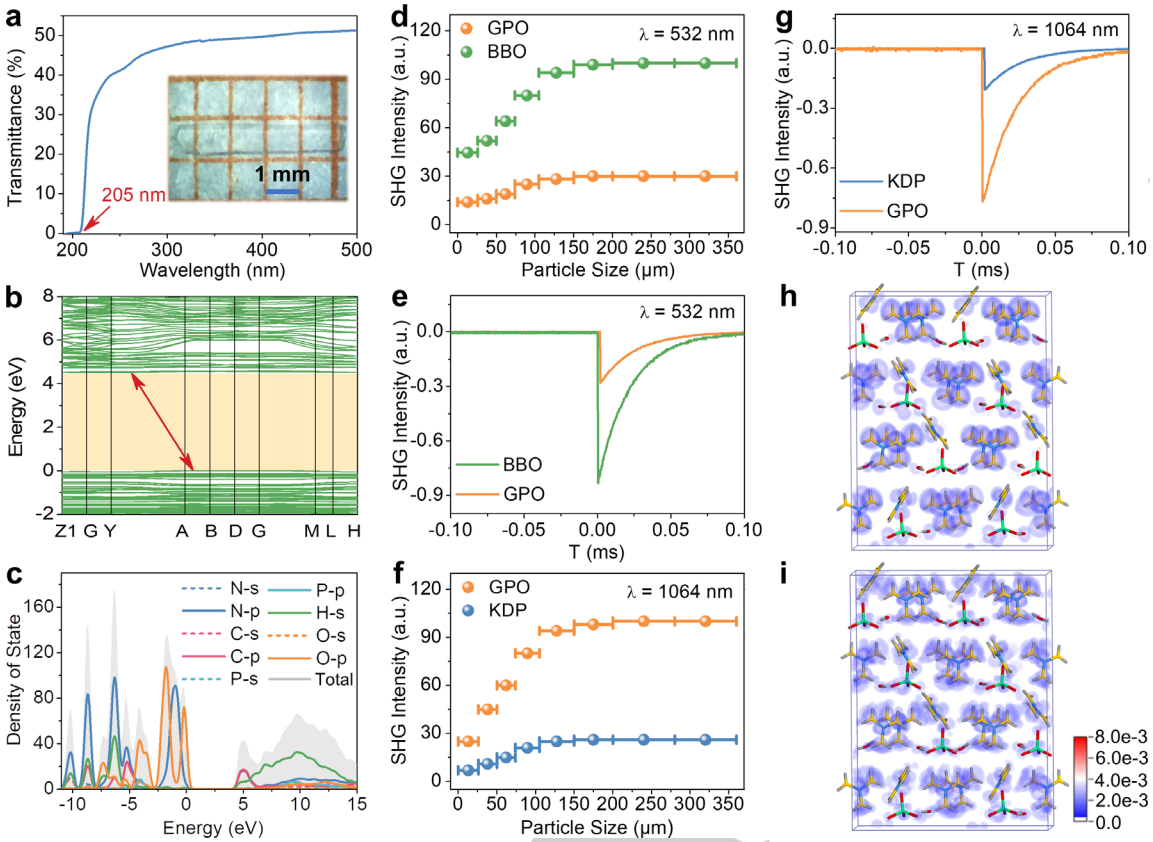

Figure 2. (a) UV transmittance spectrum of a single GPO crystal (inset: crystal photo for measurement). (b) Calculated band structure of GPO. (c) Total density of states (DOS) and partial density of states of GPO. Phase-matching curves of GPO with 532 nm (d) and 1064 nm (f) laser radiation. Oscilloscope traces of the SHG signals for powders of GPO (105−150 mm) with 532 nm (e) and 1064 nm (g) laser radiation. *β*-BBO and KDP were used as references for the SHG measurements at 532 and 1064 nm, respectively. SHG-weighted densities for (h) occupied and (i) unoccupied electronic states in GPO.

SHG-weighted electron clouds in the virtual electron (VE) process are mainly located on the $[C(NH_2)_3]^+$ cations and $[PO_4]^{3-}$ anions; for the occupied states, the SHG-weighted electron clouds are localized on the N-2p, C-2p, and O-2p orbitals, while for the unoccupied states, the N-2p, C-2p, O-2p, and P-3p orbitals make the major contribution to the SHG response. This analysis is consistent with the $[C(NH_2)_3]^+$ cations making the dominant contribution to the SHG response.

Birefringence is crucial to achieve phase-matching during the SHG process. The birefringence of GPO was measured on a polarizing microscope (ZEISS Axio Scope. A1, Figures 3a and 3b). The experimental results show that the retardation value of the measured crystal was approximately 2.098 *μ*m with a crystal thickness of 26.8 *μ*m (Figure S4), corresponding to a measured birefringence of 0.078 @ 546 nm. This birefringence is superior to those of other UV/deep-UV NLO phosphates with band gaps exceeding 6.0 eV (Table S5). The calculated dispersion of the refractive index curves of GPO reveals $n_z > n_y > n_x$, indicating that GPO is a negative biaxial crystal (Figure S5). The calculated birefringence (Δ*n*) of GPO is 0.077 @ 546 nm (Figure 3c). The shortest PM SHG wavelength is calculated to be 250 nm (Figure 3c), which is comparable to those of well-known UV NLO materials such as KDP (258 nm), LBO (277 nm), $CsLiB_6O_{10}$ (CLBO) (237 nm), and $K_3B_6O_{10}Cl$ (255 nm). To better understand the origin of the large birefringence of GPO, the real-space atom-cutting technique was also employed to evaluate the birefringence contribution (Table S6), the results confirming that the birefringence of GPO is mainly attributable to the $[C(NH_2)_3]^+$ cations (54.37% of Δ*n* @ 546 nm) and the $[PO_4]^{3-}$ anions (33.98% of Δ*n* @ 546 nm).

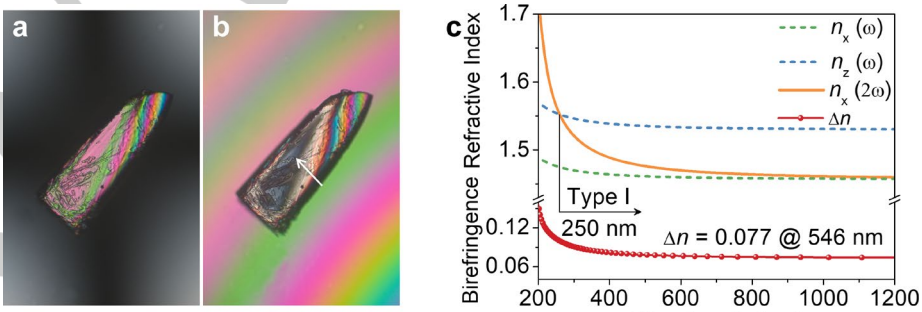

Figure 3. Comparison of (a) the original GPO crystal and (b) the GPO crystal achieving complete extinction. (c) Calculated dispersion of refractive index curves and birefringence of GPO with the shortest type-I SHG phase-matching wavelength marked.

In summary, a non-traditional π-conjugated cation $[C(NH_2)_3]^+$-based NLO phosphate, GPO, has been developed which possesses strong UV solar-blind optical nonlinearity. Unlike extant UV NLO metal phosphates, GPO possesses a short UV cutoff edge of 205 nm and shows SHG activity at both 1064 nm (3.8 × KDP) and 532 nm (0.3 × *β*-BBO). GPO also displays a large birefringence (measured: Δn = 0.078 @ 546 nm, calculated: Δn = 0.077 @ 546 nm) and short PM SHG wavelength of 250 nm, suggesting that GPO is a promising UV PM NLO material. Theoretical calculations are consistent with the remarkable linear and nonlinear optical properties of GPO mainly originating from the cooperative effect of the cationic $[C(NH_2)_3]$ planar triangles and the anionic $[PO_4]$ tetrahedra. The introduction of π-conjugated cations such as $[C(NH_2)_3]^+$ provides a new paradigm for enhancing the SHG response and birefringence of phosphate-based UV NLO materials, and should influence the development of other novel structure-driven NLO functional materials.

Acknowledgements

This research was financially supported by the National Natural Science Foundation of China (nos. 51432006, 52002276), the Ministry of Education of China for the Changjiang Innovation Research Team (no. IRT14R23), and the Ministry of Education and the State Administration of Foreign Experts Affairs for the 111 Project (no. B13025). M.G.H. thanks the Australian Research Council for support (DP170100411).

Keywords: phosphates • π-conjugated cations • ultraviolet • nonlinear optics • birefringence

[1] a) D. Cyranoski, *Nature* **2009**, *457*, 953-955; (b) P. S. Halasyamani, K. R. Poeppelmeier, *Chem. Mater.* **1998**, *10*, 2753-2769; c) N. Savage, *Nat. Photonics* **2007**, *1*, 83-85.

[2] a) M. Mutailipu, S. L. Pan, *Angew. Chem. Int. Ed.* **2020**, *59*, 20302-20317; *Angew. Chem.* **2020**, *132*, 20480-20496; b) P. S. Halasyamani, J. M. Rondinelli, *Nat. Commun.* **2018**, *9*, 2972. c) M. Luo, C. S. Lin, D. H. Lin, N. Ye, *Angew. Chem. Int. Ed.* **2020**, *59*, 15978-15981; *Angew. Chem.* **2020**, *132*, 16112-16115; d) X. H. Dong, L. Huang, C. F. Hu, H. M. Zeng, Z. E. Lin, X. Wang, K. M. Ok, G. H. Zou, *Angew. Chem. Int. Ed.* **2019**, *58*, 6528-6534; *Angew. Chem.* **2019**, *131*, 6598-6604; e) T. L. Chao, W. J. Chang, S. H. Wen, Y. Q. Lin, B. C. Chang, K. H. Lii, *J. Am. Chem. Soc.* **2016**, *138*, 9061-9064.

[3] a) J. Lu, J. N. Yue, L. Xiong, W. K. Zhang, L. Chen, L. M. Wu, *J. Am. Chem. Soc.* **2019**, *141*, 8093-8097; b) C. Wu, X. X. Jiang, Z. J. Wang, L. Lin, Z. S. Lin, Z. P. Huang, X. F. Long, M. G. Humphrey, C. Zhang, *Angew. Chem. Int. Ed.* **2021**, *60*, 3464-3468; *Angew. Chem.* **2021**, *133*, 3506-3510; c) C. Wu, T. H. Wu, X. X. Jiang, Z. J. Wang, H. Y. Sha, L. Lin, Z. S. Lin, Z. P. Huang, X. F. Long, M. G. Humphrey, C. Zhang, *J. Am. Chem. Soc.* **2021**, DOI: 10.1021/jacs.1c00416.

[4] a) P. Becker, *Adv. Mater.* **1998**, *10*, 979-992; b) T. T. Tran, H. W. Yu, J. M. Rondinelli, K. R. Poeppelmeier, P. S. Halasyamani, *Chem. Mater.* **2016**, *28*, 5238-5258; c) C. Wu, G. Yang, M. G. Humphrey, C. Zhang, *Coord. Chem. Rev.* **2018**, *375*, 459-488.

[5] a) S. G. Zhao, L. Kang, Y. G. Shen, X. D. Wang, M. A. Asghar, Z. S. Lin, Y. Y. Xu, S. S. Zeng, M. C. Hong, J. H. Luo, *J. Am. Chem. Soc.* **2016**, *138*, 2961-2964; b) T. T. Tran, J. Young, J. M. Rondinelli, P. S. Halasyamani, *J. Am. Chem. Soc.* **2017**, *139*, 1285-1295; c) G. Peng, C. C. Lin, N. Ye, *J. Am. Chem. Soc.* **2020**, *142*, 20542-20546.

[6] a) C. T. Chen, B. C. Wu, A. D. Jiang, G. M You, *Sci. Sin. B* **1985**, *15*, 235-243; b) C. T. Chen, Y. C. Wu, A. D. Jiang, B. C. Wu, G. M. You, R. K. Li, S. J. Lin, *J. Opt. Soc. Am. B* **1989**, *6*, 616-621; c) C. T. Chen, G. L. Wang, X. Y. Wang, Z. Y. Xu, *Appl. Phys. B: Lasers Opt.* **2009**, *97*, 9-25.

[7] a) G. Q. Shi, Y. Wang, F. F. Zhang, B. B. Zhang, Z. H. Yang, X. L. Hou, S. L. Pan, K. R. Poeppelmeier, *J. Am. Chem. Soc.* **2017**, *139*, 10645-10648; b) M. Luo, F. Liang, Y. X. Song, D. Zhao, F. Xu, N. Ye, Z. S. Lin, *J. Am. Chem. Soc.* **2018**, *140*, 3884-3887.

[8] a) L. Kang, F. Liang, X. X. Jiang, Z. S. Lin, C. T. Chen, *Acc. Chem. Res.* **2020**, *53*, 209-217; b) J. J. Zhou, H. P. Wu, H. W. Yu, S. T. Jiang, Z. G. Hu, J. Y. Wang, Y. C. Wu, P. S. Halasyamani, *J. Am. Chem. Soc.* **2020**, *142*, 4616-4620.

[9] a) J. H. Dang, D. J. Mei, Y. D. Wu, Z. S. Lin, *Coord. Chem. Rev.* **2021**, *431*, 213692; b) S. G. Zhao, P. F. Gong, S. Y. Luo, L. Bai, Z. S. Lin, Y. Y. Tang, Y. L. Zhou, M. C. Hong, J. H. Luo, *Angew. Chem. Int. Ed.* **2015**, *54*, 4217-4221; *Angew. Chem.* **2015**, *127*, 4291-4295.

[10] V. G. Dmitriev, G. G. Gurzadyan, D. N. Nikogosyan, *Handbook of nonlinear optical crystals*, Springer: New York, **1999**.

[11] a) P. Yu, L. M. Wu, L. J. Zhou, L. Chen, *J. Am. Chem. Soc.* **2014**, *136*, 480-487; b) J. Chen, L. Xiong, L. Chen, L. M. Wu, *J. Am. Chem. Soc.* **2018**, *140*, 14082-14086; c) H. W. Yu, J. Young, H. P. Wu, W. G. Zhang, J. Rondinelli, P. S. Halasyamani, *Chem. Mater.* **2017**, *29*, 1845-1855; d) L. Li, Y. Wang, B. H. Lei, S. J. Han, Z. H. Yang, K. R. Poeppelmeier, S. L. Pan, *J. Am. Chem. Soc.* **2016**, *138*, 9101-9104; e) Y. G. Shen, Y. Yang, S. G. Zhao, B. Q. Zhao, Z. S. Lin, C. M. Ji, L. N. Li, P. Fu, M. C. Hong, J. H. Luo, *Chem. Mater.* **2016**, *28*, 7110-7116; (f) L. Li, Y. Wang, B. H. Lei, S. J. Han, Z. H. Yang, H. Y. Li, S. L. Pan, *J. Mater. Chem. C* **2017**, *5*, 269-274; g) S. G. Zhao, X. Y. Yang, Y. Yang, X. J. Kuang, F. Q. Lu, P. Shan, Z. H. Sun, Z. S. Lin, M. C. Hong, J. H. Luo, *J. Am. Chem. Soc.* **2018**, *140*, 1592-1595; h) P. Shan, T. Q. Sun, H. D. Liu, S. G. Liu, S. L. Chen, X. W. Liu, Y. F. Kong, J. J. Xu, *Cryst. Growth Des.* **2016**, *16*, 5588-5592.

[12] S. G. Zhao, P. F. Gong, S. Y. Luo, L. Bai, Z. S. Lin, C. M. Ji, T. L. Chen, M. C. Hong, J. H. Luo, *J. Am. Chem. Soc.* **2014**, *136*, 8560-8563.

[13] a) T. T. Tran, N. Z. Koocher, J. M. Rondinelli, P. S. Halasyamani, *Angew. Chem. Int. Ed.* **2017**, *56*, 2969-2973; *Angew. Chem.* **2017**, *129*, 3015-3019; b) M. Mutailipu, M. Zhang, H. P. Wu, Z. H. Yang, Y. H. Shen, J. L. Sun, S. L. Pan, *Nat. Commun.* **2018**, *9*, 3089-3098.

[14] a) G. H. Zou, N. Ye, L. Huang, X. Lin, *J. Am. Chem. Soc.* **2011**, *133*, 20001-20007; b) T. T. Tran, J. G. He, J. M. Rondinelli, P. S. Halasyamani, *J. Am. Chem. Soc.* **2015**, *137*, 10504-10507.

[15] X. M. Liu, P. F. Gong, Y. Yang, G. M. Song, Z. S. Lin, *Coord. Chem. Rev.* **2019**, *400*, 213045.

[16] a) H. W. Yu, J. Young, H. P. Wu, W. G. Zhang, J. M. Rondinelli, P. S. Halasyamani, *J. Am. Chem. Soc.* **2016**, *138*, 4984-4989; b) C. Wu, L. Lin, X. X. Jiang, Z. S. Lin, Z. P. Huang, M. G. Humphrey, P. S. Halasyamani, C. Zhang, *Chem. Mater.* **2019**, *31*, 10100-10108.

[17] a) Y. L. Deng, L. Huang, X. H. Dong, L. Wang, K. M. Ok, H. M. Zeng, Z. E. Lin, G. H. Zou, *Angew. Chem. Int. Ed.* **2020**, *59*, 21151-21156; *Angew. Chem.* **2020**, *132*, 21337-21342; b) H. W. Yu, W. G. Zhang, J. Young, J. M. Rondinelli, P. S. Halasyamani, *J. Am. Chem. Soc.* **2016**, *138*, 88-91; c) X. F. Lu, Z. H. Chen, X. R. Shi, Q. Jing, M. H. Lee, *Angew. Chem. Int. Ed.* **2020**, *59*, 17648-17656; *Angew. Chem.* **2020**, *132*, 17801-17809; d) M. Abudoureheman, S. J. Han, B. H. Lei, Z. H. Yang, X. F. Long, S. L. Pan, *J. Mater. Chem. C* **2016**, *4*, 10630-10637; e) L. Qi, Z. H. Chen, X. R. Shi, X. D. Zhang, Q. Jing, N. Li, Z. Q. Jiang, B. B. Zhang, M. H. Lee, *Chem. Mater.* **2020**, *32*, 8713-8723; f) C. Wu, L. H. Li, L. Lin, Z. P. Huang, M. G. Humphrey, C. Zhang, *Chem. Mater.* **2020**, *32*, 3043-3053; g) C. Wu, X. X. Jiang, L. Lin, Z. S. Lin, Z. P. Huang, M.G. Humphrey, C. Zhang, *Chem. Mater.* **2020**, *32*, 6906-6915.

[18] B. L. Wu, C. L. Hu, F. F. Mao, R. L. Tang, J. G. Mao, *J. Am. Chem. Soc.* **2019**, *141*, 10188-10192.

[19] C. T. Chen, G. Z. Liu, *Annu. Rev. Mater. Sci.* **1986**, *16*, 203-243. (b) C. T. Chen, R. K. Li, *Int. Rev. Phys. Chem.* **1989**, *8*, 65-91.

[20] G. H. Zou, L. Huang, N. Ye, C. S. Lin, W. D. Cheng, H. Huang, *J. Am. Chem. Soc.* **2013**, *135*, 18560-18566.

[21] R. W. Godby, M. Schlüter, L. J. Sham, *Phys. Rev. B: Condens. Matter Mater. Phys.* **1987**, *36*, 6497-6500.

[22] W. Kohn, *Rev. Mod. Phys.* **1999**, *71*, 1253-1266.

[23] a) J. Lin, M. H. Lee, Z. P. Liu, C. T. Chen, C. J. Pickard, *Phys. Rev. B* **1999**, *60*, 13380-13389; b) R. He, Z. S. Lin, M. H. Lee, C. T. Chen, *J. Appl. Phys.* **2011**, *109*, 103510.

Entry for the Table of Contents

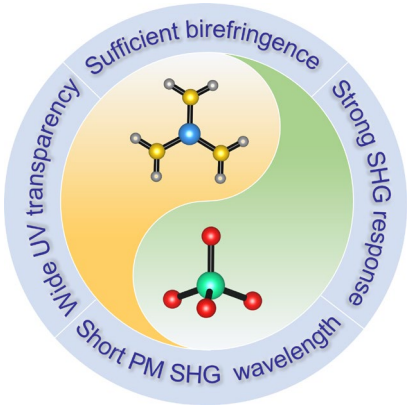

The π-conjugated cation-based phosphate $[C(NH_2)_3]_6(PO_4)_2 \cdot 3H_2O$ exhibits rare coexistence of wide UV transparency, large second harmonic generation (SHG) response and sufficient birefringence for phase-matching at a short SHG wavelength.